

Optical magnetic circular dichroism in threshold photoemission from a magnetite thin film

This article has been downloaded from IOPscience. Please scroll down to see the full text article.

2008 J. Phys.: Condens. Matter 20 235218

(<http://iopscience.iop.org/0953-8984/20/23/235218>)

View [the table of contents for this issue](#), or go to the [journal homepage](#) for more

Download details:

IP Address: 129.252.86.83

The article was downloaded on 29/05/2010 at 12:32

Please note that [terms and conditions apply](#).

Optical magnetic circular dichroism in threshold photoemission from a magnetite thin film

K Hild¹, J Maul^{1,3}, T Meng¹, M Kallmayer¹, G Schönhense¹,
H J Elmers¹, R Ramos², S K Arora² and I V Shvets²

¹ Institut für Physik, Johannes Gutenberg-Universität, Staudinger Weg 7,
D-55128 Mainz, Germany

² Centre for Research on Adaptive Nanostructures and Nanodevices (CRANN),
School of Physics, Trinity College Dublin, Dublin 2, Republic of Ireland

E-mail: jmaul@uni-mainz.de

Received 12 December 2007, in final form 9 April 2008

Published 6 May 2008

Online at stacks.iop.org/JPhysCM/20/235218

Abstract

Threshold photoemission excited by polarization-modulated ultraviolet femtosecond laser light is exploited for phase-sensitive detection of magnetic circular dichroism (MCD) for a magnetite thin film. Magnetite (Fe_3O_4) shows a magnetic circular dichroism of $\sim(4.5 \pm 0.3) \times 10^{-3}$ for perpendicularly incident circularly polarized light and a magnetization vector switched parallel and antiparallel to the helicity vector by an external magnetic field. The asymmetry in threshold photoemission is discussed in comparison to the magneto-optical Kerr effect. The optical MCD contrast in threshold photoemission will provide a basis for future laboratory photoemission studies on magnetic surfaces.

(Some figures in this article are in colour only in the electronic version)

1. Introduction

With the availability of ultrashort pulse lasers covering the complete visible and near ultraviolet range, laser probes became indispensable for the study of surface magnetism, achieving extended spectroscopic analysis and unprecedented time resolution. By the use of intense laser light, threshold photoemission gives direct access to the electronic structure in the vicinity of the Fermi level [1–3], despite the decreasing quantum efficiency.

In contrast to the magneto-optical Kerr effect (MOKE), only those transitions from levels below the Fermi energy which contribute to the emission of photoelectrons are averaged, i.e. averaging of many transitions is avoided. Magnetic circular dichroism (MCD) in threshold photoemission thus provides information on a strongly restricted region in k space at the Γ point and close to the Fermi level, which is very interesting for transport properties. In addition, exploiting magnetic dichroism in threshold photoemission appears promising for high magnetic contrasts, especially in the

presence of strong spin–orbit coupling for states directly below the Fermi level. Threshold photoemission can be further exploited for magnetic imaging studies using photoemission electron microscopy (PEEM), where the chromatic error is kept at a minimum due to the small energy distribution of the emitted photoelectrons. The resulting lateral resolution is expected to be in the range of ~ 50 nm [3] which is superior to the resolution obtained with optical Kerr microscopy.

So far, threshold photoemission has been applied to the study magnetic dichroism by only a few groups after its theoretical prediction by Feder *et al* [4]. Marx *et al* [5] demonstrated magnetic linear dichroism (MLD) in PEEM using a high-pressure mercury arc-lamp and optical filters (photon energies $h\nu < 5.2$ eV). Nakagawa *et al* [6, 7] made use of table-top lasers at fixed photon energy for the measurement of both magnetic linear and MCD, thereby attaining high MCD asymmetries above 10% for Ni(100). In contrast to synchrotron-based x-ray magnetic circular dichroism (XMCD, [8–10]) which profits from the strong spin–orbit coupling of atomic core levels, the mechanisms for threshold magnetic dichroism are more subtle because of the absence of discrete atomic levels.

³ Author to whom any correspondence should be addressed.

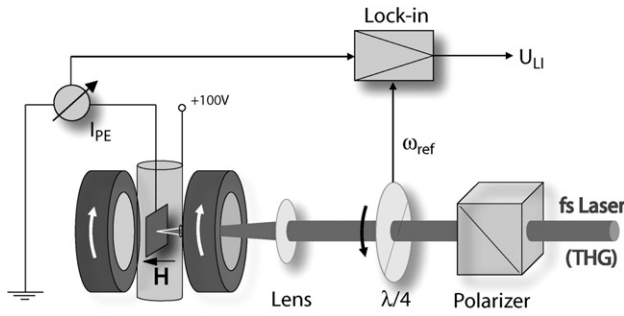


Figure 1. Schematic view of the photoemission experiment: third harmonic generation (THG) from a Ti:Sa femtosecond laser is used for a polarization-sensitive detection of the photoemission current from perpendicularly magnetized samples. MCD asymmetries in the photoemission are obtained by comparing the amplified photocurrent upon irradiation with circularly polarized UV light of different helicity.

In the present work, we use the total photoelectron yield (TEY) from femtosecond laser-excited threshold photoemission to measure MCD in a perpendicularly magnetized magnetite thin film. For the measurement of small magnetic effects, the method presented utilizes phase-sensitive photocurrent detection in the presence of periodically modulated laser polarization and is similar to the approach chosen by Nagakawa *et al* [6]. Unlike synchrotron experiments with a complex instrumentation, this method offers a simple laboratory probe for surface magnetism with potential for future studies with higher time resolution.

2. Experiment

The experimental setup is schematically shown in figure 1: frequency-tripled radiation from a femtosecond Ti:Sa laser (MaiTai, Spectra Physics; $\lambda_{3\omega} = 267$ nm, $h\nu = 4.64$ eV) passes a Glan–Thompson polarizer for proper definition of the linear polarization vector relative to a subsequent quarter-wave plate. The quarter-wave plate is built into a rotatable motor mount which rotates at a frequency $\omega_{\text{ref}}/2\pi = 10$ Hz and periodically modulates the polarization with a frequency $2\omega_{\text{ref}}$. The modulated laser light is slightly focused ($f = 500$ mm) onto a thin film sample at normal incidence. The sample is kept under high vacuum ($p \sim 10^{-7}$ mbar) and placed in the gap of a commercial electromagnet with brace insertions (not explicitly shown) generating a homogeneous magnetic field at the sample position of up to 1.6 T. The total photoelectron yield (TEY) is measured by a picoammeter (Keithley Instruments Picoammeter 6485) recording the photocurrent upon laser irradiation via the sample current. A bias voltage of +100 V is applied to a cylindrical counter electrode to extract the photoemission current.

For polarization-sensitive detection of the photocurrent, the voltage output from the picoammeter is used as input signal for a lock-in amplifier (EG&G Princeton Applied Research, Model 5207) for phase-sensitive measurement of the $2\omega_{\text{ref}}$ -intensity modulation. By optimizing the phase adjustment of the lock-in amplifier, the photocurrent modulation that is

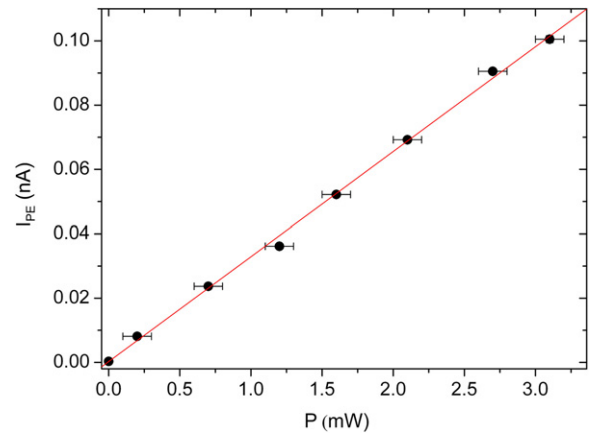


Figure 2. Photoemission current recorded from the magnetite thin film sample in dependence of the ultraviolet laser power at 267 nm wavelength.

caused by the polarization modulation of the light is selectively recorded at a low signal-to-noise ratio.

3. Results

A 100 nm thick $\text{Fe}_3\text{O}_4(111)$ layer grown on $\text{Al}_2\text{O}_3(0001)$ by oxygen plasma assisted molecular beam epitaxy [11, 12] was used for the study of magnetic dichroism in threshold photoemission. The back side of the substrate was fixed to the sample mount by UHV compatible silver glue ensuring conductive contact to the sample surface.

The dependence of the photoemission yield from the ultraviolet laser irradiance was measured directly by means of the implemented picoammeter. Throughout the experiment, the dimensions of the sample (5 mm \times 10 mm) notably exceeded the laser spot size (~ 3 mm²). In figure 2 we plot the measured sample current versus the incident laser power. The linear dependence of the observed TEY current demonstrates that the signal is dominated by one-photon absorption; multiphoton contributions are negligible in the presence of the chosen laser fluences. The photon energy of 4.64 eV (corresponding to a wavelength of $\lambda = 267$ nm) is nominally smaller than the work function of a clean $\text{Fe}_3\text{O}_4(111)$ surface ($\phi = [5.52 \pm 0.05]$ eV, [13]). However, the surface has not been cleaned prior to the experiment and it is known that the work function of $\text{Fe}_3\text{O}_4(111)$ strongly decreases upon chemisorption. A typical saturation value for the work function decrease is -1.2 eV [13], resulting in a photoemission threshold of ~ 4.3 eV. This explains the observed linear behavior of the photoemission current. The quantum efficiency (QE) given by the photoelectrons recorded per incident photon is obtained from the slope of the straight line, $\text{QE} \sim 1.6 \times 10^{-7}$. This small value is explained by the strong restriction on energy and momentum for photoelectrons emitted near the photoemission threshold. In turn, this restriction on energy and momentum space represents an essential criterion for high MCD signals in threshold photoemission which are expected in the presence

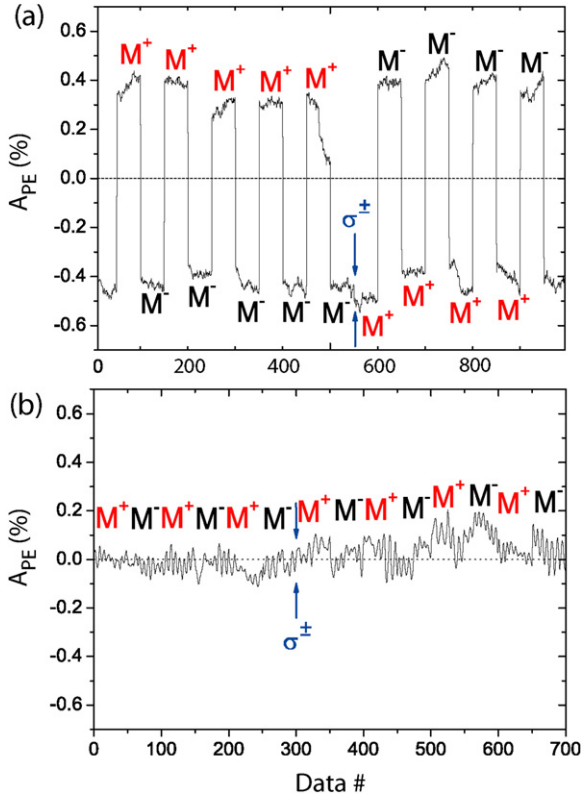


Figure 3. (a) Measurement sequence for verification of the MCD asymmetry A_{PE} in the photoemission from the magnetite thin film sample, based on reversals in the magnetization orientation M^\pm and in changes of the photon helicity σ^\pm . The arrows indicate simultaneous change in the magnetization orientation and in the photon helicity. (b) The same measurement sequence applied to a tantalum sample.

of strong spin-orbit splitting at the Γ point directly below the Fermi level, as is fulfilled for magnetite for example [14].

We use polarization-modulated UV laser light to measure asymmetries in the photoemission yield depending on the helicity of the circular polarization relative to the magnetization vector. Measurement sequences are defined by alternating magnetic field reversals together with helicity changes of the circular polarization. MCD is primarily confirmed by two criteria: (1) periodic changes in the TEY following periodic changes in the magnetization orientation parallel or antiparallel to the laser beam, and (2) constancy in the TEY during a simultaneous change of both the magnetic field orientation and the helicity of the circular polarization.

Figure 3(a) depicts such a measurement sequence. Magnetization parallel and antiparallel to the incident laser beam is denoted by M^+ and M^- , respectively. The helicities of the circular polarization are labeled σ^\pm , corresponding to two different lock-in phase settings for the polarization-selective amplification of the photocurrent signal. The magnetic field was set to $\mu_0 H = \pm 1.05$ T, and the laser power was 3 mW throughout the MCD experiment. In order to display the magnetic asymmetry in photoemission

$$A_{PE} = \frac{I_{PE}^+ - I_{PE}^-}{I_{PE}^+ + I_{PE}^-} \approx \frac{I_{PE}^+ - I_{PE}^-}{2I_{PE}} \quad (1)$$

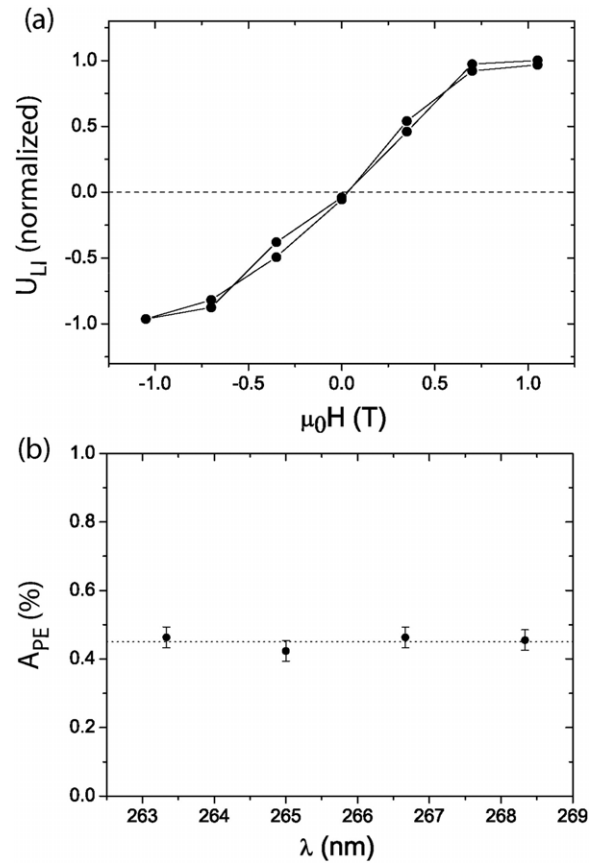


Figure 4. Parametric study of the magnetite thin film MCD asymmetry. (a) Magnetization curve obtained from the normalized lock-in output under magnetic field variation (from $\mu_0 H = +1.05$ T to $\mu_0 H = -1.05$ T and reverse). The magnetization saturates at about $\mu_0 H_S \sim 0.8$ T. (b) Wavelength independence of the MCD asymmetry near the photoemission threshold. The average of $A_{PE} = 0.45\%$ is indicated as a dashed line.

directly, the lock-in voltage output was referred to the corresponding photocurrent averages I_{PE}^+ , I_{PE}^- over each segment of alternating magnetization M^+ , M^- . For the investigated magnetite sample, the MCD asymmetry is determined to $A_{PE} = (4.5 \pm 0.3) \times 10^{-3}$. The integration time for each data point was 1 s. A waiting time of 30 s was used for each magnetic field reversal. Hence, the data points do not directly translate into measurement time.

In addition, a (nonmagnetic) tantalum surface was also investigated. For this nonmagnetic sample the dichroic signal vanishes within an uncertainty of $A_{PE} \sim 1 \times 10^{-3}$, as can be seen from figure 3(b). Here, the lock-in signal was formally translated into an MCD asymmetry.

Further evidence for the MCD effect is provided by the magnetization curve shown in figure 4(a): because the magnetite film shows an in-plane easy axis, the magnetization vector reversibly rotates from an in-plane direction to the film normal with increasing field. The coercive field and the hysteresis vanish. A saturation magnetization of $\mu_0 H_S \sim 0.75$ T is extracted which lies below the magnetic field applied for the measurement sequence in figure 3(a).

The different absorption of circularly polarized light of opposite helicity can be explained using the polar magneto-

optical Kerr effect (MOKE). In metal optics in the regime of visible light the circular dichroism in absorption is related to the Kerr ellipticity in polar geometry. However, this model does not consider that only a small fraction of absorbed photons leads to photoemitted electrons. The threshold photoemission intensity is determined by only those transitions exciting electrons close to the Fermi edge within the energy interval between E_F and $E_F - h\nu + \phi$, whereas in magneto-optics a broad energy interval between E_F and $E_F - h\nu$ contributes. The MCD asymmetry in threshold photoemission can in principle, but not necessarily, be much larger than magneto-optical Kerr effects because fewer transitions contribute and thus less averaging takes place.

For comparison, the MCD asymmetry A_K determined in reflection from polar MOKE measurements with circularly polarized light is directly related to the polar Kerr ellipticity ε_K of the reflected light. This is calculated within the Jones formalism for reflected light from a magnetic surface at normal incidence, where the complex Kerr angle $\Psi_K = \Theta_K + i\varepsilon_K$ changes the electric field vector $\vec{E}_{\sigma\pm} = (E_x, E_y) = (1, \pm i)$ by:

$$\begin{pmatrix} E'_x \\ E'_y \end{pmatrix} = \begin{pmatrix} 1 & \Psi_K \\ \Psi_K & -1 \end{pmatrix} \begin{pmatrix} E_x \\ E_y \end{pmatrix}. \quad (2)$$

The MCD asymmetry results in twice the negative polar Kerr ellipticity:

$$A_K = \frac{|\vec{E}'_{\sigma\pm}|^2 - |\vec{E}'_{\sigma\mp}|^2}{|\vec{E}'_{\sigma\pm}|^2 + |\vec{E}'_{\sigma\mp}|^2} = \frac{-2\varepsilon_K}{1 + |\Psi_K|^2} \approx -2\varepsilon_K. \quad (3)$$

Leonov *et al* [14] performed LSDA + U calculations for the polar Kerr ellipticity at a photon energy of $h\nu = 4.5$ eV for magnetite, yielding $\varepsilon_K = -0.043^\circ$ and $A_K = 1.5 \times 10^{-3}$. However, the experimental data for the polar Kerr ellipticity at $h\nu = 4.5$ eV yielded $\varepsilon_K = -0.15^\circ$ for magnetite [14] which translates into a significantly larger reflection MCD asymmetry of $A_K = 5.2 \times 10^{-3}$.

To be more specific, the comparison between polar MOKE asymmetry involving the reflected light intensity I_R and photoemission MCD asymmetry involving the absorbed light intensity $I_A = I_0 - I_R$ needs to be discussed in a complementary way by writing the polar Kerr asymmetry A_K in terms of the absorbed intensity I_A :

$$A_K \cong \frac{I_R^+ - I_R^-}{2I_R} = -\frac{I_A^+ - I_A^-}{2I_R}. \quad (4)$$

This is related to the MCD asymmetry in absorption, given by

$$A_A := \frac{I_A^+ - I_A^-}{2I_A}, \quad (5)$$

which depends on the ratio between reflected and absorbed intensity:

$$A_A = -A_K \frac{I_R}{I_A}. \quad (6)$$

To a first approximation, we assume that the absorbed intensity I_A is proportional to the total photoemission yield I_{PE} , $I_A \propto I_{PE}$. In this case, the proportionality factor cancels in equation (5), resulting in $A_{PE} = A_A$. Expressing the

reflected and the absorbed intensity in terms of the reflectivity R , $I_R = RI_0$, and $I_A = (1 - R)I_0$, the photoemission MCD asymmetry A_{PE} is given by:

$$A_{PE} = -A_K \left(\frac{R}{1 - R} \right). \quad (7)$$

Using the reflectivity of $R = 0.21$ for magnetite at a photon energy of $h\nu = 4.64$ eV [15], a photoemission MCD asymmetry of $A_{PE} = 1.4 \times 10^{-3}$ is obtained using the experimental value for ε_K , respectively $A_{PE} = 3.4 \times 10^{-4}$ using the calculated value of ε_K . The photoemission MCD asymmetry $A_{PE} = (4.5 \pm 0.3) \times 10^{-3}$ determined within our experiment at a photon energy of $h\nu = 4.64$ eV significantly exceeds these values. This can be interpreted by additional enhancements of the MCD signal due to selection in energy and momentum space expected in threshold photoemission, as explained above.

For future work, the use of tunable lasers will enable extended spectroscopic studies of photoemission near the Fermi level. In a first measurement, we tuned the UV laser light by $\delta\lambda \sim 5$ nm around $\lambda = 267$ nm, corresponding to a narrow energy interval of $\delta E \sim 90$ meV (figure 4(b)). However, this interval is sufficient to allow for a basic comparison with the results discussed in [6], where an increase in the excitation energy of ~ 100 meV in the direct vicinity of the photoemission threshold leads to a significant decrease in the MCD asymmetry due to strong changes in the band structure near the Fermi level. In our case, we do not observe a significant change of the asymmetry in this energy range. This might be seen as a hint that band structure changes affect the MCD signal more strongly for Ni(100) compared to magnetite in (sub-)threshold photoemission.

4. Conclusion and outlook

Ultraviolet optical MCD in the photoemission from a magnetite thin film was shown using polarization-modulated laser light and phase-sensitive photocurrent detection. The photoemission MCD asymmetry amounts to $A_{PE} \sim (4.5 \pm 0.3) \times 10^{-3}$. This value was compared to MOKE data for magnetite, showing that threshold photoemission gives rise to an enhanced MCD signal. Future work aims at the application of femtosecond laser magnetic dichroism for time-resolved pump probe photoemission studies.

Acknowledgment

The experiment was funded by the DFG, EL-172/12-3.

References

- [1] Fanelisa A, Kisker E, Henk J and Feder R 1996 *Phys. Rev. B* **54** 2922
- [2] Knorren R, Bennemann K H, Burgermeister R and Aeschlimann M 2000 *Phys. Rev. B* **61** 9427
- [3] Schönhense G 1999 *J. Phys.: Condens. Matter* **11** 9517
- [4] Feder R, Henk J and Johansson B 1998 *Solid State Commun.* **108** 713

- [5] Marx G K L, Elmers H J and Schönhense G 2000 *Phys. Rev. Lett.* **84** 5888
- [6] Nakagawa T and Yokoyama T 2006 *Phys. Rev. Lett.* **96** 237402
- [7] Nakagawa T, Yokoyama Y, Hosaka M and Katoh M 2007 *Rev. Sci. Instrum.* **78** 023907
- [8] Schütz G, Wagner W, Wilhelm W, Kienle P, Zeller R, Frahm R and Materlik G 1987 *Phys. Rev. Lett.* **58** 737
- [9] Marangolo M, Gustavsson F, Eddrief M, Sainctavit Ph, Etgens V H, Cros V, Petroff F, George J M, Bencok P and Brookes N B 2002 *Phys. Rev. Lett.* **88** 217202
- [10] Schneider C M and Schönhense G 2002 *Rep. Prog. Phys.* **65** R1785
- [11] Arora S K, Sofin R G S, Shvets I V and Luysberg M 2006 *J. Appl. Phys.* **100** 073908
- [12] Kallmayer M, Hild K, Elmers H J, Arora S K, Wu H C, Sofin R G S and Shvets I V 2008 *J. Appl. Phys.* **103** 07D715
- [13] Weiss W and Ranke W 2002 *Prog. Surf. Sci.* **70** 1
- [14] Leonov I, Yaresko A N, Antonov V N and Anisimov V I 2006 *Phys. Rev. B* **74** 165117
- [15] Schlegel A, Alvarado S F and Wachter P 1978 *J. Phys. C: Solid State Phys.* **12** 1157